Electrochemical and Spectroelectrochemical Investigations of $[(TpTP)M^{V}L_2]^{+}Cl^{-}$ Where TpTP Is the Dianion of Tetra-*p*-tolylporphyrin, M = P or Sb, and L = Cl^{-} or OCH_3^{-}

Y. H. Liu,[1a] M.-F. Bénassy,[1a] Stephen Chojnacki,[1a] Francis D'Souza,[1a] Tanya Barbour,[1b] Warwick J. Belcher,[1b] Penelope J. Brothers,*[,1b] and Karl M. Kadish*[,1a]

Departments of Chemistry, University of Houston, Houston, Texas 77204-5641, and University of Auckland, Private Bag, Auckland, New Zealand

Received May 4, 1994[⊗]

The electrochemical and spectroelectrochemical properties of $[(TpTP)M^{V}(L)_2]^{+}Cl^{-}$ in dichloromethane are presented where M = P or Sb, L = OCH_3^{-} or Cl^{-}, and TpTP is the dianion of tetra-*p*-tolylporphyrin. All four porphyrins undergo two one-electron reductions on the cyclic voltammetry time scale to give initially porphyrin π anion radicals and dianions. The singly and doubly reduced products of $[(TpTP)M^{V}(OCH_3)_2]^{+}Cl^{-}$ are relatively stable, but this is not the case for the two $[(TpTP)M^{V}Cl_2]^{+}Cl^{-}$ complexes, both of which undergo a series of chemical reactions following electron transfer. The coupled electrochemical/chemical reactions lead to a low-valent M(III) complex in the case of the bis(chloro) Sb(V) derivative and to numerous decomposition products, including the free base porphyrin, in the case of the bis(chloro) P(V) porphyrin. UV-visible spectroelectrochemical and EPR data suggest that the four investigated porphyrins all undergo an internal charge transfer from the electrogenerated porphyrin π anion radical to the Sb(V) or P(V) porphyrin center. The EPR spectrum of singly reduced $[(TpTP)Sb^{V}Cl_2]^{+}Cl^{-}$ at 123 K in CH_2Cl_2 has a signal centered at $g = 2.018$ and exhibits hyperfine splitting due to interaction between the metal and the unpaired electron on the porphyrin macrocycle. The three other singly reduced porphyrins display a specturm with broad isotropic signals centered at $g \sim 2.00$ and a spectral line width which increases with temperature, also supporting an internal charge transfer mechanism.

Introduction

Relatively few porphyrins containing group 15 elements were synthesized and characterized over the last two decades,[2-16] but several of these complexes were recently utilized as photosensitizers for electron transfer[17-21] and oxygenation reactions.[22,23] Two oxidation states, +5 and +3, are available to each group 15 metalloporphyrin, and each has a characteristic UV-visible spectrum. The high-valent complexes, represented as $[(Por)M^{V}L_2]^{+}$, where L is an anionic axial ligand and Por is the dianion of a given porphyrin macrocycle, have what are called "normal UV-visible absorption spectra" and are characterized by a single Soret band located at 390-430 nm.[11] This contrasts with the low-valent group 15 metalloporphyrins which are represented as $[(Por)M^{III}]^{+}$ and show "irregular p-type hyper absorption spectra", i.e., a split Soret band with maxima in the regions 350-380 and 440-480 nm, respectively.[11,24] These latter types of spectral features are also seen for metalloporphyrins in Nature. For example, the UV-vis spectrum of cytochrome P_{450}-CO has a split Soret band and has been used to study the orbital interactions which produce these hyper-type spectra.[25,26]

The accessibility of two central metal oxidation states in group 15 metalloporphyrins suggests that one should be able to measure the redox potentials for conversion between a high and low oxidation state form of the porphyrin, but this is not the case, despite speculation that this should occur.[4,6] For example, two reversible electroreductions are seen for antimony(V) and antimony(III) octaethylporphyrins,[8] but both sets of electrode reactions involve the porphyrin π-ring system. An internal charge transfer from a doubly reduced P(V) porphyrin dianion to the central metal of the complex has been proposed,[4,6] but this has never been experimentally demonstrated. In fact, a transient species has yet to be detected upon reduction of any

[⊗] Abstract published in *Advance ACS Abstracts,* September 1, 1994.

(1) (a) University of Houston. (b) University of Auckland.
(2) Barbour, T.; Belcher, W. J.; Brothers, P. T.; Rikard, C. E. F.; Ware, D. C. *Inorg. Chem.* **1992**, *31*, 746.
(3) Buchler, J. K.; Lay, K. L. *Inorg. Nucl. Chem. Lett.* **1974**, *10*, 297.
(4) Carrano, C. J.; Tsutsui, M. *J. Coord. Chem.* **1977**, *9*, 79.
(5) Marrese, C. A.; Carrano, C. J. *J. Chem. Soc., Chem. Commun.* **1982**, 1279.
(6) Marrese, C. A.; Carrano, C. J. *Inorg. Chem.* **1983**, *22*, 1858.
(7) Marrese, C. A.; Carrano, C. J. *Inorg. Chem.* **1984**, *23*, 3961.
(8) Connell, C. R. Ph.D. Thesis, Department of Chemistry, University of Washington, Seattle, 1977.
(9) Sayer, P.; Gouterman, M.; Connell, C. R. *J. Am. Chem. Soc.* **1977**, *99*, 1082.
(10) Gouterman, M.; Sayer, P.; Shankland, E.; Smith, J. P. *Inorg. Chem.* **1981**, *20*, 87.
(11) Sayer, P.; Gouterman, M.; Connell, C. R. *Acc. Chem. Res.* **1982**, *15*, 73.
(12) Treibs, A. *Liebigs Ann. Chem.* **1969**, *728*, 115.
(13) Mangani, S.; Meyer, E. F.; Cullen, D. L.; Tsutsui, M.; Carrano, C. J. *Inorg. Chem.* **1983**, *22*, 401.
(14) Iitzgerald, A.; Stenkamp, R. E.; Watenpaugh, K. D.; Jensen, L. H. *Acta Crystallogr.* **1977**, *1333*, 1688.
(15) Marrese, C. A.; Cavrano, C. J. *J. Chem. Soc., Chem. Commun.* **1982**, 1279.
(16) Segawa, H.; Nakayama, N.; Shimidzu, T. *J. Chem. Soc., Chem. Commun.* **1992**, 784.
(17) Shelnutt, J. A. *J. Am. Chem. Soc.* **1983**, *105*, 7179.
(18) Shelnutt, J. A. *J. Phys. Chem.* **1984**, *88*, 6121.
(19) Shelnutt, J. A. U.S. Patent 4568435, 1986.
(20) Kalyanasundaram, K.; Shelnutt, J. A.; Gratzel, M. *Inorg. Chem.* **1988**, *27*, 2820.
(21) Segawa, J.; Kunimoto, K.; Nakamoto, A.; Shimidzu, T. *J. Chem. Soc., Perkin Trans. 1* **1992**, 939.
(22) Okamoto, T.; Takagi, S.; Shiragami, T.; Inoue, H. *Chem. Lett.* **1993**, 687.
(23) Takagi, S.; Okamoto, T.; Shiragami, T.; Inoue, H. *Chem. Lett.* **1993**, 793.
(24) Knör, G.; Vogler, A. *Inorg. Chem.* **1994**, 33, 314.
(25) Hanson, L. K.; Eaton, W. A.; Sligar, S. G.; Gunsalus, I. C.; Gouterman, M.; Connell, C. R. *J. Am. Chem. Soc.* **1976**, *98*, 2672.
(26) Dawson, J. H.; Trudell, J. R.; Barth, G.; Linder, R. E.; Bunnenberg, E.; Djerassi, C.; Gouterman, M.; Connell, C. R.; Sayer, P. *J. Am. Chem. Soc.* **1977**, *99*, 641.

0020-1669/94/1333-4480$04.50/0

[(Por)P^{V}L$_2$]$^+$ complex, perhaps because the electroreduction results in demetalation leading to formation of the free base porphyrin, (Por)H$_2$.[4,6]

Antimony(III) porphyrins are known to be relatively more stable than their phosphorus(III) analogs;[11] thus an internal charge transfer between the porphyrin π anion radical or dianion and the central metal of the electroreduced Sb(V) derivative might be spectroscopically observable. This is indeed the case as shown in the present paper, which reports the electrochemistry of [(TpTP)M^V(OCH$_3$)$_2$]$^+$Cl$^-$ and [(TpTP)M^{V}Cl$_2$]$^+$Cl$^-$, where M = P or Sb and TpTP is the dianion of tetra-*p*-tolylporphyrin. The compounds exist in ionic forms in solution and are henceforth represented as [(TpTP)M^V(L)$_2$]$^+$ where M = Sb or P and L = Cl$^-$ or OCH$_3^-$. The site of electron transfer during electroreduction was determined using UV−visible and EPR measurements. The influence of the central metal ion and coordinated axial ligands on the redox potentials and stability of the electroreduced products is described.

Experimental Section

Chemicals. HPLC grade methylene chloride (CH_2Cl_2) was distilled over P_2O_5. Tetrabutylammonium perchlorate (TBAP), used as supporting electrolyte, was twice recrystallized from absolute ethanol and stored under vacuum at 40 °C. The syntheses of [(TpTP)P(OCH$_3$)$_2$]$^+$Cl$^-$, [(TpTP)PCl$_2$]$^+$Cl$^-$, [(TpTP)Sb(OCH$_3$)$_2$]$^+$Cl$^-$, and [(TpTP)SbCl$_2$]$^+$Cl$^-$ have been previously described.[2]

Instrumentation. EPR spectra were recorded in frozen solution with a Bruker ESP 300 or ER 100D spectrometer. Thin-layer electronic absorption spectra were recorded with a Tracor Northern Model 6500 multichannel spectrometer. Platinum working and counter electrodes were used for all electrochemical measurements. A saturated calomel electrode (SCE) was used as a reference electrode and was separated from the bulk of the solution by a fritted-glass disk junction. The thin-layer spectroelectrochemical cell was previously described.[27] Cyclic voltammograms were recorded with a three-electrode system using an EG&G 174A potentiostat coupled with an EG&G 175 universal programmer, an IBM EC 225 voltammetric analyzer, or a BAS 100 electrochemical analyzer. Bulk controlled-potential coulometry was performed with an EG&G 173 potentiostat−galvanostat.

Results and Discussion

Electroreduction of [(TpTP)P(OCH$_3$)$_2$]$^+$ and [(TpTP)PCl$_2$]$^+$. Room-temperature electrochemistry of [(TpTP)PL$_2$]$^+$ in CH_2Cl_2, 0.2 M TBAP is dependent upon the nature of the coordinated axial ligand, L, as shown in Figure 1. The bis(methoxy) derivative, [(TpTP)P(OCH$_3$)$_2$]$^+$, undergoes two reversible one-electron reductions (labeled as processes I and II) at $E_{1/2}$ = −0.55 and −1.09 V. Two major reductions are also seen for the bis(chloro) derivative, [(TpTP)PCl$_2$]$^+$, the first of which is reversible if the scan is reversed at −0.50 V (see dashed line in Figure 1b). The second reduction is irreversible at room temperature but not at low temperature as shown in Figure 1b.

The room-temperature voltammogram of [(TpTP)PCl$_2$]$^+$ displays several peaks at potentials negative of the cathodic peak II which are attributed to one or more products generated from the homogeneous chemical reaction(s) following the second electron transfer (*vide infra*). These reactions can be slowed at −75 °C, and under these conditions, processes I and II are reversible. However, a new low-temperature redox couple is seen at $E_{1/2}$ = −1.4 V vs SCE. The peak currents for this process are small compared to those for the first two reductions, and the origin of this electrode reaction is not clear; it may involve a further reduction of the porphyrin macrocycle or possibly a reduction of the P(V) ion but was not further investigated in the present study.

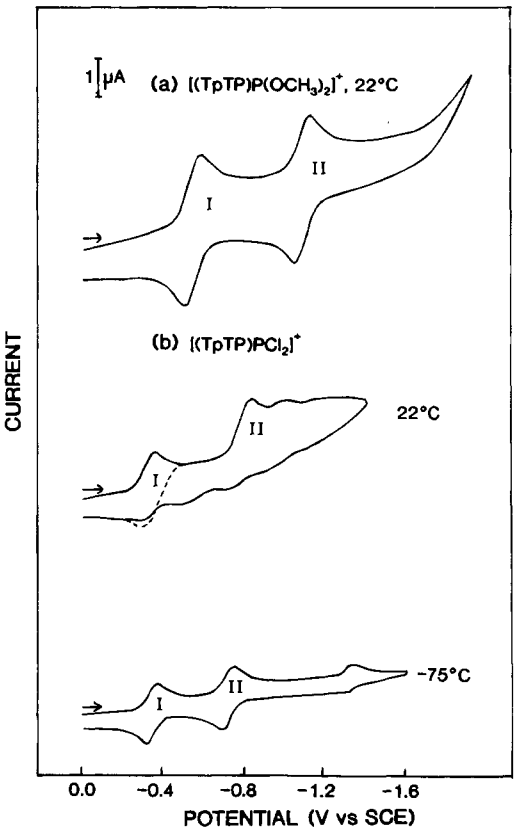

Figure 1. Cyclic voltammograms of (a) [(TpTP)P(OCH$_3$)$_2$]$^+$ at 22 °C and (b) [(TpTP)PCl$_2$]$^+$ at 22 and −75 °C in CH_2Cl_2, 0.2 M TBAP.

Table 1. Half-Wave Potentials for the Reduction of [(TpTP)PL$_2$]$^+$ and [(TpTP)SbL$_2$]$^+$ (L = OCH$_3^-$, Cl$^-$) in CH_2Cl_2, 0.2 M TBAP

		$E_{1/2}$ (V vs SCE)	
complex	temp (°C)	I	II
[(TpTP)P(OCH$_3$)$_2$]$^+$	20	−0.55	−1.09
	−75	−0.56	−1.02
[(TpTP)PCl$_2$]$^+$ [a]	20	−0.33	−0.79[b]
	−75	−0.34	−0.72
[(TpTP)Sb(OCH$_3$)$_2$]$^+$	20	−0.42	−0.90
	−75	−0.42	−0.81
[(TpTP)SbCl$_2$]$^+$ [a]	20	−0.26	−0.52[b]
	−75	−0.29	−0.55[b]

[a] Additional reductions are observed at more negative potentials and are due to the generated chemical products. [b] E_p at a scan rate of 0.1 V/s.

Thin-layer UV−vis spectra were recorded during the first two controlled-potential reductions of each compound in CH_2Cl_2. The resulting UV−vis spectral data are given in Table 2, which also lists the applied reduction potential. As the first controlled-potential reduction of [(TpTP)P(OCH$_3$)$_2$]$^+$ proceeds at −0.80 V, the original absorption bands at 432, 560, and 603 nm decrease in intensity and new broad bands diagnostic of a porphyrin π anion radical[28,29] appear between 650 and 800 nm. The second reduction of [(TpTP)P(OCH$_3$)$_2$]$^+$ results in a further decrease and broadening of both the Soret and visible bands, consistent with formation of a porphyrin dianion.[28]

Similar spectral changes are observed during the stepwise controlled-potential electrolysis of [(TpTP)PCl$_2$]$^+$ at −0.44 V. The initial Soret band at 442 nm decreases in intensity and undergoes a blue shift of 4 nm as the first reduction proceeds. The emergence of a new broad absorption band at 740 nm is

(27) Lin, X. Q.; Kadish, K. M. *Anal. Chem.* **1985**, *57*, 1498.
(28) Felton, R. H. In *The Porphyrins*; Dolphin, D., Ed.; Academic Press: New York, 1979; Vol. IV, pp 53−115.
(29) Kadish, K. M.; Tagliatesta, P.; Hu, Y.; Deng, Y. J.; Mu, X. H.; Bao, L. Y. *Inorg. Chem.* **1991**, *30*, 3737.

Table 2. Maximum Absorbance Wavelengths and Corresponding Molar Absorptivities of $[(TpTP)P(L)_2]^+$ and $[(TpTP)Sb(L)_2]^+$ (L = OCH_3^-, Cl^-) before and after Reduction in CH_2Cl_2, 0.2 M TBAP

complex	appl pot. (V)	λ, nm (ε)						
$[(TpTP)P(OCH_3)_2]^+$	none		432 (324)		560 (17)	603 (6.5)		
	−0.80		437 (107)				665 (16.2)	710 (17.8)
	−1.30	323 (61)	423 (67)		581 (22)			
$[(TpTP)PCl_2]^+$	none		442 (267)		570 (13.6)	615 (9.6)		
	−0.44	350 (36)	438 (134)					740 (11.3)
	−0.90[a]		420 (58.7)	458 (40.6)				
	−1.28		419 (44.7)					
$[(TpTP)Sb(OCH_3)_2]^+$	none		424 (557)		552 (23)	595 (20)		
	−0.60		429 (111)					710 (6.8)
	−1.20		418 (108)		554 (3.1)			
$[(TpTP)SbCl_2]^+$	none		430 (384)		558 (29.3)	602 (30.3)		
	−0.40[b]	367 (46.9)	432 (233)	468 (67.2)	561 (9.6)	606 (14.0)		703 (15.7)
	−0.40[c]	362 (68.4)		468 (310)		604 (13.3)	652 (22.8)	
	−0.80[d]	360 (51.6)	420 (177)	442 (29.0)	473 (60.7)		647 (11.6)	825 (18.7)

[a] Weak absorptions are also seen at 511, 551, 592, and 648 nm. [b] Recorded after 10 s. [c] Recorded after 5 min. [d] Generation of $(TpTP)Sb^{III}$ π anion radical prior to demetalation.

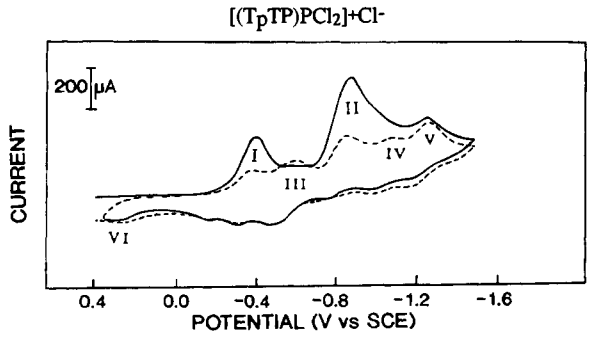

Figure 2. Thin-layer cyclic voltammograms of $[(TpTP)PCl_2]^+$ in CH_2Cl_2 containing 0.2 M TBAP for the first (—) and second (- - -) potential scans.

characteristic of a ring-centered electroreduction. Further controlled-potential reduction at −0.90 V leads to a species with a greatly reduced Soret band intensity and five new bands (λ = 420, 511, 551, 592, 648 nm) assigned to demetalated free base $(TpTP)H_2$. Other absorptions are also seen at 458 and 820 nm and are attributed to the presence of a phlorin anion.[30,31]

Similar assignments for the electroreduction products can be made on the basis of results from multiple-scan, thin-layer cyclic voltammetry. Processes I and II of $[(TpTP)PCl_2]^+$ are well-defined on the initial cathodic potential scan (solid line, Figure 2), but the second scan (dashed line) is characterized by three new peaks labeled as III−V. Process V at $E_{1/2} = -1.21$ V is associated with the first reduction of free base $(TpTP)H_2$. There is also a small irreversible oxidation peak at $E_p = 0.28$ V (process VI) which is attributed to oxidation of the chemically generated phlorin anion.[6] The second potential sweep exhibits electrochemical behavior similar to that of the phlorin anion generated from (TPP)Zn in DMF during electroreduction.[31] However, the potentials for processes III and IV of $[(TpTP)PCl_2]^+$ are both anodically shifted from those for reduction of the (TPP)Zn phlorin anion presumably due to the different inductive effects of the Zn(II) and P(V) ions.

The singly reduced products of $[(TpTP)P(OCH_3)_2]^+$ and $[(TpTP)PCl_2]^+$ both have isotropic EPR signals and g values centered around 2.00 over a temperature range of 23 to −150 °C. The spectral line widths, ΔH, are found to be 1.92 G for $[(TpTP)P(OCH_3)_2]^+$ and 5.14 G for $[(TpTP)PCl_2]^+$ at −150 °C. These values increase with temperature and reach maxima of 9.46 G for $[(TpTP)P(OCH_3)_2]^+$ and 8.11 G for $[(TpTP)PCl_2]^+$ at 23 °C (see Table 3). It is known that EPR spectra of metalloporphyrin π anion radicals with electroinactive central metals such as zinc[32,33] have ΔH values which do not broaden with increase in temperature. The observation of this phenomenon for singly reduced $[(TpTP)PL_2]^+$ suggests an interaction between the unpaired electron on the macrocycle and the central phosphorus nucleus. The spectroelectrochemical data in Table 2 indicate that the initial site of reduction is the conjugated porphyrin macrocycle and not the central metal, and an internal charge transfer must therefore be the route for formation of any P(III) complex if it is indeed formed.

Table 3. EPR Parameters for the One-Electron-Reduced Products of the Phosphorus(V) and Antimony(V) Porphyrins in CH_2Cl_2, 0.2 M TBAP

	T = 23 °C		T = −150 °C	
complex	g	ΔH_{pp} (G)	g	ΔH_{pp} (G)
$[(TpTP)P(OCH_3)_2]^+$	2.003	9.46	2.002	1.92
$[(TpTP)PCl_2]^+$	2.005	8.11	2.001	5.14
$[(TpTP)Sb(OCH_3)_2]^+$	2.004	48.65	1.999	19.46
$[(TpTP)SbCl_2]^+$	2.004[a]	5.95[a]	2.018	$a(^{121}Sb) = 63.5$ $a(^{123}Sb) = 35.1$

[a] At −196 °C.

Electroreduction of $[(TpTP)Sb(OCH_3)_2]^+$ and $[(TpTP)SbCl_2]^+$. Cyclic voltammograms illustrating the reduction of $[(TpTP)Sb(OCH_3)_2]^+$ and $[(TpTP)SbCl_2]^+$ in CH_2Cl_2 are shown in Figure 3. The reversible processes I and II of $[(TpTP)Sb(OCH_3)_2]^+$ are located at $E_{1/2} = -0.42$ and −0.90 V, values which are shifted in a positive direction by −130 to −190 mV as compared to $E_{1/2}$ for the two electroreductions of $[(TpTP)P(OCH_3)_2]^+$. This is not unexpected due to the stronger inductive effect of Sb(V) as compared to P(V).

The room-temperature electrochemical behavior of $[(TpTP)SbCl_2]^+$ (Figure 3a) is different from that of $[(TpTP)PCl_2]^+$ (Figure 1b) in that the products of the second electroreduction seem to be well defined on the cyclic voltammetry time scale. Process I of $[(TpTP)SbCl_2]^+$ is reversible and located at $E_{1/2} = -0.26$ V when the potential scan is reversed at −0.4 V (dashed line) but irreversible when the scan is reversed at potentials negative of process II. Two additional, reversible reductions are then seen at $E_{1/2} = -0.60$ and −0.97 V and assigned to reduction of one or more porphyrin products generated from the homogeneous chemical reaction following the second electron transfer. The final product in solution is stable on the

(30) Peychal-Heiling, G.; Wilson, G. S. *Anal. Chem.* **1971**, *43*, 550.
(31) Lanese, J. G.; Wilson, G. S. *J. Electrochem. Soc.* **1972**, *119*, 1039.
(32) Fajer, J.; Davis, M. S. In *The Porphyrins*; Dolphin, D., Ed.; Academic Press: New York, **1979**; Vol. IV, pp 197−256.
(33) Seth, J.; Bocian, D. F. *J. Am Chem. Soc.* **1994**, *116*, 143.

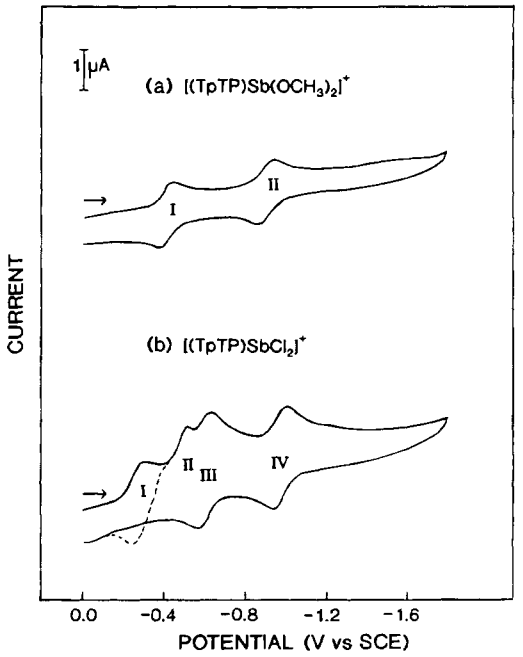

Figure 3. Cyclic voltammograms of (a) $[(TpTP)Sb(OCH_3)_2]^+$ and (b) $[(TpTP)SbCl_2]^+$ in CH_2Cl_2 containing 0.2 M TBAP.

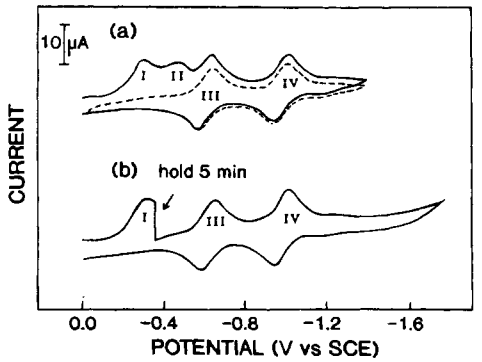

Figure 4. Thin-layer cyclic voltammograms of $[(TpTP)SbCl_2]^+$ in CH_2Cl_2 containing 0.2 M TBAP (a) for the first (—) and second (- - -) potential scans and (b) for a single scan where the potential is held negaive of the first reduction (−0.40 V for 5 min).

cyclic voltammetry time scale as demonstrated by the multiple-scan, thin-layer cyclic voltammogram in Figure 4. Processes I and II are seen only on the first negative potential scan while processes III and IV are the major electrode reactions seen on all further potential sweeps.

The same chemical species seems to be formed following the first or second reduction of $[(TpTP)SbCl_2]^+$, as suggested by the voltammograms in Figure 4 and the spectroelectrochemical data in Figure 5. In Figure 4b, the potential was held at −0.40 V during the initial cathodic scan, which resulted in an almost complete loss of the currents for process II and fully developed processes III and IV. The UV−visible spectrum recorded during the first 10 s of electrolysis at the same applied potential initially exhibits absorption bands characteristic of a porphyrin π anion radical[28,29] (Figure 5a), but these bands disappear at longer times and a new hyper-type spectrum is then observed (Figure 5b). This spectrum, which has a split Soret band at 362 and 468 nm and two visible bands at 604 and 652 nm, is assigned to an Sb(III) porphyrin on the basis of a comparison with spectral data in the literature for other group 15 porphyrins with +3 central metal ions.[2,24] For example, the UV−vis spectrum in Figure 5b is almost identical to the spectrum reported for $(TpTP)Bi^{III}NO_3$ in CH_2Cl_2 (λ_{max} = 354, 469, 601, 650 nm).[2] The ratio of molar absorptivities between the 469 and 354 nm Soret bands of the Bi(III) complex is 3.93.

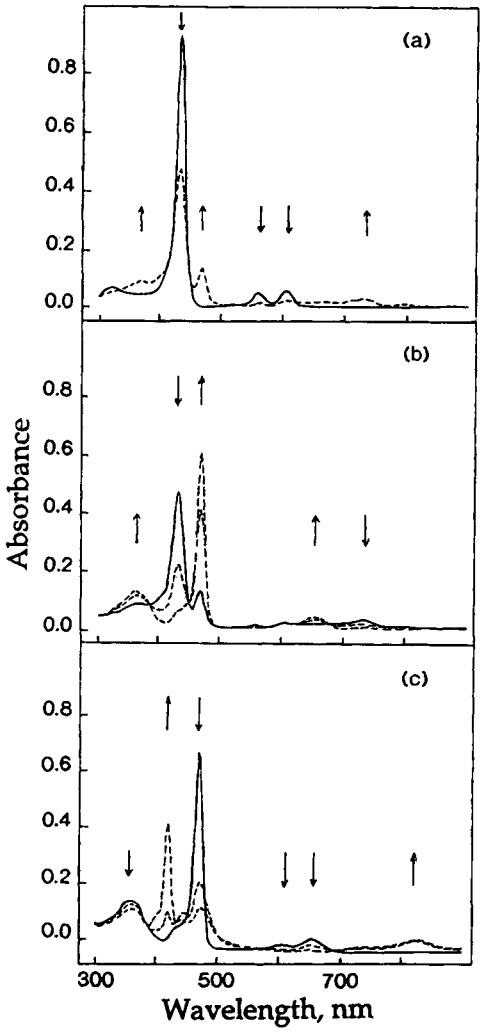

Figure 5. Time-dependent UV−visible spectral changes obtained during the controlled-potential reduction of $[(TpTP)SbCl_2]^+$ in CH_2Cl_2 containing 0.2 M TBAP (a) during the first 10 s at −0.40 V (process I), (b) at longer time scales at −0.40 V, and (c) at −0.80 V (process II).

The same ratio for the chemical reduction product of $[(TpTP)SbCl_2]^+$, using the absorbances at 468 and 362 nm, is 4.53. Consequently, the product of the chemical reaction in Figure 5b is assigned to $[(TpTP)Sb^{III}]^+$, which has a p-type hyper absorption spectrum. On the other hand, as mentioned above, the initial UV−visible spectrum obtained during controlled-potential reduction at an applied potential negative of process I (Figure 5a) indicates that the electron transfer first involves the porphyrin π-ring system. A continued application of the applied potential gives the Sb(III) complex as a final porphyrin product, and the same chemical species is also formed after the second reduction of $[(TpTP)SbCl_2]^+$, as shown in Figures 3b and 4a. A combination of these results thus leads to the overall mechanism shown in Scheme 1 where L = OCH_3^- or Cl^-.

The reversible one-electron reductions labeled as processes III and IV in Scheme 1 occur at $E_{1/2}$ = −0.60 and −0.97 V and are assigned to reduction of the *in situ* generated $[(TpTP)Sb^{III}]^+$. The Sb(V) complex most likely loses the two axially bound Cl^- ligands either prior to or during the internal electron transfer reaction to give the Sb(III) species. A similar loss of axial ligands has been proposed during electroreduction of $[(Por)P^{V}Cl_2]^+$,[5-7] but this is followed by rapid demetalation, perhaps due to an instability of the resulting P(III) porphyrin complex.

The spectral changes observed during the controlled-potential electrolysis of $[(TpTP)SbCl_2]^+$ at −0.80 V, i.e., a potential

Scheme 1

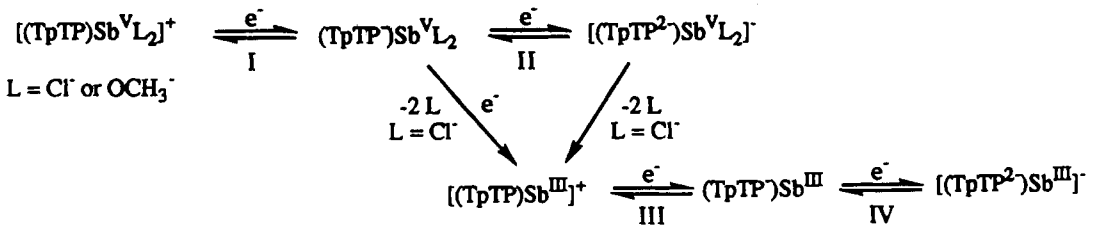

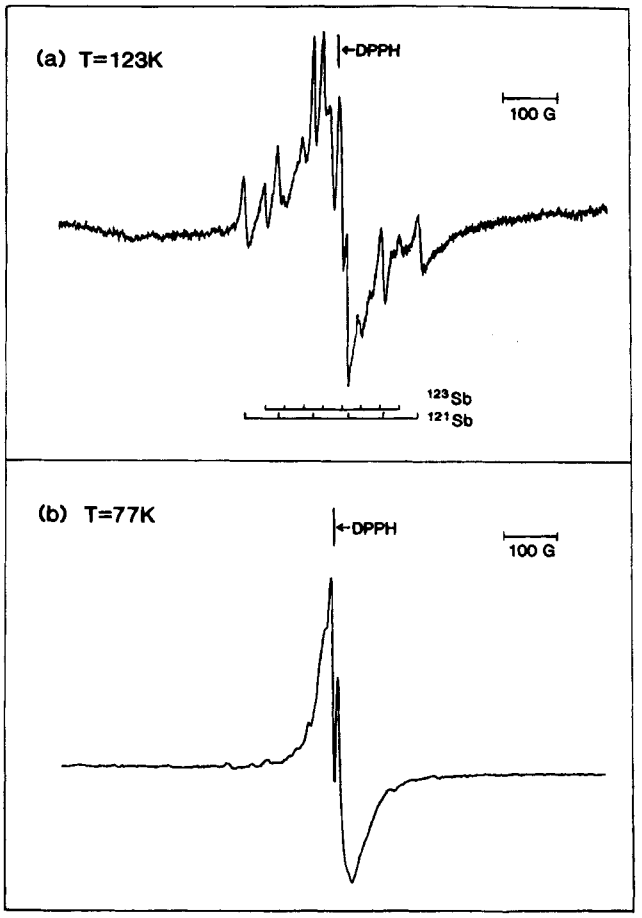

Figure 6. ESR spectra obtained at (a) 123 K and (b) 77 K after the bulk controlled-potential reduction of $[(TpTP)SbCl_2]^+$ at −0.40 V for 3 min in CH_2Cl_2, 0.2 M TBAP.

negative of process III, are given in Figure 5c. The initial spectrum obtained at this potential shows a decreased intensity Soret band and a broad absorption band between 700 and 900 nm indicative of a π anion radical.[28] The appearance of a new Soret band at 420 nm and weak absorptions between 500 and 650 nm in the final spectrum are indicative of the formation of free base porphyrin, $(TpTP)H_2$. These results suggest that $[(TpTP)Sb^{III}]^+$ does not undergo demetalation but that the electroreduced π anion radical, $(TpTP^-)Sb^{III}$, does. Thin-layer coulometry of $[(TpTP)SbCl_2]^+$ shows the transfer of 2.0 ± 0.1 electrons upon reduction at −0.54 V, suggesting that the chemical reaction product is generated from the electroreduced species. In contrast to the bis(chloro) Sb(V) complex, $[(TpTP)Sb(OCH_3)_2]^+$ can be converted to both a stable π anion radical and dianion during the first and second one-electron reductions. No chemical reactions are seen on the thin-layer cyclic voltammetric time scale, and the spectral data of the reduction products are summarized in Table 2.

Figure 6 depicts EPR signals obtained at two different temperatures after bulk controlled-potential electrolysis of $[(TpTP)Sb^{V}Cl_2]^+$ at −0.40 V for 3 min. The spectrum at −150 °C (Figure 6a) shows hyperfine splitting from both the ^{121}Sb ($I = {}^5/_2$) and ^{123}Sb ($I = {}^7/_2$) nuclei but becomes less well-defined when the temperature is lowered to −196 °C (Figure 6b), at which point the signal becomes almost isotropic. This suggests that the unpaired electron is localized on the macrocycle at −196 °C but distributed onto the antimony central ion at higher temperatures; i.e., there is a temperature-dependent charge transfer between the reduced porphyrin ring and metal ion as shown in eq 1.

$$\underset{\text{(low temp)}}{(TpTP^-)Sb^{V}Cl_2} \rightleftharpoons \underset{\text{(high temp)}}{(TpTP)Sb^{IV}Cl_2} \qquad (1)$$

An analysis of the EPR spectrum in Figure 6a shows a hyperfine coupling constant of 63.5 G originating from an interaction of the unpaired electron with the ^{121}Sb nucleus. A similar interaction with the ^{123}Sb nucleus leads to a coupling constant of 35.1 G.

The EPR spectrum of singly reduced $[(TpTP)Sb(OCH_3)_2]^+$ shows a broad signal whose g value is centered around 2.00 (see Table 3). The spectral line width of this signal is maximum at room temperature (ΔH = 48.6 G) and steadily decreases to 19.5 G at −150 °C. Hyperfine coupling originating from an interaction of the unpaired electron with the antimony nucleus is not observed over a temperature range of +23 to −150 °C. The increase in ΔH values with temperature for singly reduced $[(TpTP)Sb(OCH_3)_2]^+$ suggests an interaction between the unpaired electron on the macrocycle and the central antimony nucleus and is seen for the phosphorus complexes.

In summary, we have shown how the coordinated axial ligands on $[(TpTP)M^{V}(L)_2]^+$ will affect the electrochemical behavior of the complexes. The two investigated bis(methoxy) porphyrins are both stable upon electroreduction; this contrasts with the two bis(chloro) derivatives, which undergo a series of chemical reactions leading either to a low-valent porphyrin in the case of antimony or a demetalated product in the case of phosphorus. The higher stability of the methoxy derivatives suggests that these ligands stabilize the higher oxidation state of the group 15 central ions, an effect also observed for other transition metal porphyrins.[34,35] The data suggest that the two methoxy ligands remain bound to the metal center after the first and second electroreduction at the porphyrin π-ring system whereas the two chloride ligands are most likely lost; this is the key point in defining both the resulting electrochemistry and the ultimate reaction products. The ligand loss seems to facilitate the internal electron transfer which eventually leads to a metal(III) derivative.

Acknowledgment. The support of the Robert A. Welch Foundation (K.M.K., Grant E-680), The University of Houston Energy Lab, and the National Science Foundation is gratefully acknowledged.

(34) Swistak, C.; Mu, X. H.; Kadish, K. M. *Inorg. Chem.* **1987**, *26*, 4360.
(35) Kadish, K. M. *Prog. Inorg. Chem.* **1986**, *34*, 435.